

# Identification of Armature, Field, and Saturated Parameters of a Large Steam Turbine-Generator from Operating Data

H. Bora Karayaka, Ali Keyhani, Baj L. Agrawal, Douglas A. Selin, and Gerald Thomas Heydt

**Abstract**—This paper presents a step by step identification procedure of armature, field and saturated parameters of a large steam turbine-generator from real time operating data. First, data from a small excitation disturbance is utilized to estimate armature circuit parameters of the machine. Subsequently, for each set of steady state operating data, saturable mutual inductances  $L_{ads}$  and  $L_{aqs}$  are estimated. The recursive maximum likelihood estimation technique is employed for identification in these first two stages. An artificial neural network (ANN) based estimator is later used to model these saturated inductances based on the generator operating conditions. Finally, using the estimates of the armature circuit parameters, the field winding and some damper winding parameters are estimated using an Output Error Method (OEM) of estimation. The developed models are validated with measurements not used in the training of ANN and with large disturbance responses.

**Index Terms**—Parameter identification, large utility generators, saturation modeling, artificial neural networks, field winding degradation, state estimation.

## I. INTRODUCTION

ON-LINE parameter identification for large synchronous generators is a beneficial procedure which does not require any service interruption to perform. Thus, machine parameters, which can deviate during on-line operation at different loading levels due to saturation, internal temperature and machine aging can be determined without costly testing [1]. Also, an accurate stability analysis requires the precise modeling of generator saturation—a complex phenomenon involving loading conditions, excitation levels and the machine power angle. The saturation can be significant both in the direct and quadrature axes [2]. Accurate models for machine saturation analysis can be found in references [2]–[10]. In most of these studies, the independent variables used in modeling nonlinear variations of the saturation factors are primarily the terminal voltage, current or a combination of these quantities including the phase angle. Due to the complexity of the saturation phenomenon, only some of the physical factors are taken into consideration in these studies.

In this study, data sets acquired at different loading and excitation levels of a large utility generator are utilized to identify

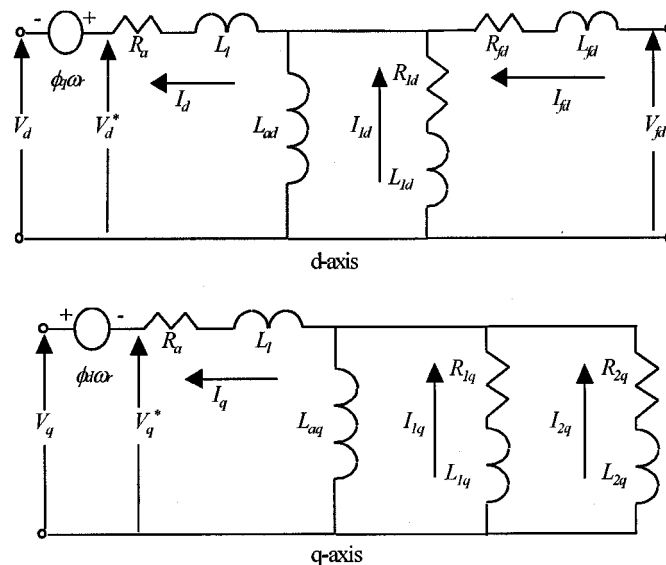


Fig. 1. On-line model structure.

the machine parameters. It is assumed that the machine model order is known (i.e. the number of differential equations). Estimated mutual inductances for each operating point are then mapped into operating condition dependent machine variables using artificial neural networks. By collecting data from various loading and excitation levels, the span of these machine variables representing various operating points is kept wide enough so that this multi-dimensional non linear mapping is able to generalize the estimates for the data points not included in training. The ANN can easily identify the shape of the nonlinear function from training data. Therefore no apriori knowledge of the shape of the mapping is required. A similar study can be found in reference [15] for a small salient pole synchronous generator. Based on the ANN estimator developed for saturated mutual inductances, field winding and direct axis damper winding parameters are identified from large excitation disturbance data.

## II. MACHINE MODEL DESCRIPTION AND PROBLEM FORMULATION

The structure of the synchronous machine model used in this study is a standard second order model with one damper in the  $d$ -axis and two dampers in the  $q$ -axis given in Fig. 1 [1]. For

Manuscript received November 6, 1998; revised March 16, 1999. This work was supported in part by the National Science Foundation, Grant ECS9722844.

H. B. Karayaka and A. Keyhani are with Ohio State University, Department of Electrical Engineering, Columbus, OH.

B. L. Agrawal and D. A. Selin are with Arizona Public Service Company, Phoenix, AZ.

G. T. Heydt is with Arizona State University, Tempe, AZ.

Publisher Item Identifier S 0885-8969(00)04520-4.

continuous time systems, the state space representation of this model is,

$$\begin{aligned} dX(t)/dt &= A(\theta) \cdot X(t) + B(\theta) \cdot U(t) + w(t) \\ Y(t) &= C \cdot X(t) + v(t) \end{aligned} \quad (1)$$

where  $w(t)$  and  $v(t)$  represent the process and measurement noise. Also,

$$\begin{aligned} X &= [i_q \ i_d \ i_{1q} \ i_{2q} \ i_{1d} \ i_{fd}^*]^t; \\ U &= [v_q \ v_d \ v_{fd}^*]^T; \\ Y &= [i_q \ i_d \ i_{fd}^*]^T; \\ \theta &= [R_a \ R_{fd}^* \ R_{1d} \ L_1 \ L_{ad} \ L_{fd} \ L_{1d} \ a \ R_{1q} \ R_{2q} \ L_{aq} \ L_{1q} \ L_{2q}]^T. \end{aligned}$$

All parameters are in actual units. Also, it is assumed that the machine power angle  $\delta$  is available for measurement. Variables  $v_d, v_q, i_d, i_q$  represent generator  $d$ - and  $q$ -axis terminal voltages and currents respectively. The quantities  $i_{fd}^*$  and  $v_{fd}^*$  represent field current and field voltage respectively as measured on the field side of the generator and  $R_{fd}^*$  is the field winding resistance as measured on the field side. Terms  $i_{fd}, v_{fd}$  and  $R_{fd}$  represent corresponding transformed quantities on the stator side through the field to stator turns ratio  $a = N_{fd}/N_s$  as follows,

$$i_{fd} = \frac{2}{3} a i_{fd}^*; \quad v_{fd} = \frac{v_{fd}^*}{a}; \quad R_{fd} = \frac{3}{2} \frac{1}{a^2} R_{fd}^*.$$

All other variables and parameters are referred to the stator.

The machine parameters including armature, field and saturated parameters are identified in five stages:

- Measurement data validation.
- Using small excitation disturbance data, estimation of armature circuit parameters including  $a$ .
- Estimation of saturated mutual inductances  $L_{ads}$  and  $L_{aqs}$  for each steady state operating point by fixing  $R_a$  and  $a$  from previous estimation.
- Development of ANN model for mapping  $L_{ads}$  and  $L_{aqs}$  to various operating points.
- Estimation of field winding and  $d$ -axis damper winding parameters using estimated parameters from previous steps.

In order to validate the established model based on estimated parameters, simulation studies are performed and the results are compared against actual measurements under large excitation disturbances. In these studies, measured terminal voltage and field voltage are used to excite the machine model to obtain terminal current and field current. The simulated currents are compared against corresponding actual measurements.

### III. MEASUREMENT DATA VALIDATION

The large steam turbine-generator used for study purposes was Four Corners Unit 5. This unit is a participant owned unit which is operated by Arizona Public Service Co. (APS). The measurement data provided by APS was validated for consistency before attempting to use it in estimation procedure. The following quantities were verified:

*Line voltages and phase currents:* Since the unit has a high grounding impedance, the following should be satisfied,

$$\begin{cases} i_{as} + i_{bs} + i_{cs} = 0 \\ v_{as} + v_{bs} + v_{cs} = 0 \end{cases} \quad (2)$$

However, due to measurement offset problems this was not found to be exactly true. The computations show that there exists a small and consistent value for each test case which is clearly a sign of biased measurements or measurement offsets. This offset is evenly distributed and subtracted from each measurement. In addition, phase order for both phase currents and line voltages were verified.

*Active power and power factor angle:* Once the line voltages and phase currents are validated and corrected, the active power and power factor angle can be considered for validation. For a balanced system,

$$P_0(t) = i_a(t)v_{ab}(t) - i_c(t)v_{bc}(t) \quad (3)$$

$$P_{ss} = \frac{3}{2} V_t I_t \cos \phi \quad (4)$$

In equation (3) all quantities are instantaneous. Equation (4) is steady state formulation of three phase active power where the  $V_t, I_t$  are terminal voltage and current peak values respectively and  $\phi$  is the power factor angle. These quantities are calculated and compared for steady state portions of each test case to validate  $\phi$  and  $P_{ss}$ . The results show that there is good agreement between these quantities.

*Power angle,  $\delta$ :* The steady state value of power angle, is calculated using the following relation:

$$E_q \angle \delta = V_t \angle 0 + I_t \angle \phi (R_a + jX_q) \quad (5)$$

Using the known values of  $V_t, I_t$ , and  $\phi$ , and the manufacturer supplied values of  $R_a, X_q$ , the power angle is computed and compared against the measured steady state value of  $\delta$  (the measured value of  $\delta$  was obtained from a special power angle measurement device [22]). A consistent offset was present between calculated and measured value of  $\delta$ . This offset was recognized from the test data when the  $\delta$  angle should be zero to correspond with zero measured active power.

It is important to note that, estimation of  $L_q$  is very sensitive to the accuracy of  $\delta$  for small angles. Because, at steady state (if the contribution of  $R_a$  is ignored)

$$V_d = V_t \sin \delta \cong V_t \delta = X_q I_q. \quad (6)$$

As can be seen from relation (6), a one degree error in measured  $\delta$ , can cause significant errors in estimated  $X_q$  or  $L_q$ .

*Field voltage and current  $v_{fd}^*, i_{fd}^*$ :* For each test case, the ratio  $v_{fd}^*/i_{fd}^*$  for each steady state operating point is compared against  $R_{fd}^*$  provided by manufacturer. The results show that there is a good agreement between these two quantities.

### IV. ESTIMATION OF ARMATURE CIRCUIT PARAMETERS

The first stage of the estimation process involves estimation of linear armature circuit parameters of the machine. In order

TABLE I  
LINEAR MODEL PARAMETER ESTIMATES FOR DIFFERENT VALUES OF  $R_a$

Parameters (mH)	Estimates for $R_a=0.0023\Omega$	Estimates for $R_a=0.0046\Omega$	Estimates for $R_a=0.0069\Omega$
$aL_{ad}$	57.5813	57.5833	57.5853
$L_d$	3.9775	3.9780	3.9785
$L_q$	3.5068	3.4702	3.4336

to satisfy linearity, the field side of the machine should be disturbed in small amounts (about 2 to 5%) so that the change in parameters is minimal. The measurements needed for the estimation process are  $v_{ab}, v_{bc}, v_{ca}, i_{as}, i_{bs}, i_{cs}, i_{fd}^*$  and  $\delta$ . These quantities can be converted to  $dq$  axis equivalents by following the steps described in reference [14].

The following model which is used for estimation of armature circuit parameters can be established in terms of  $dq$  axis variables assuming the damper winding currents and the rate of change of stator flux linkages is zero,

$$\begin{bmatrix} v_d \\ v_q \end{bmatrix} = \begin{bmatrix} -i_d & 0 & \omega_r i_q & 0 \\ -i_q & \frac{2}{3}\omega_r i_{fd}^* & 0 & -\omega_r i_d \end{bmatrix} \begin{bmatrix} R_a \\ aL_{ad} \\ L_q \\ L_d \end{bmatrix} + \begin{bmatrix} v_1 \\ v_2 \end{bmatrix}. \quad (7)$$

The above equation is in the form of  $Y = H\theta + V$ , where,  $Y = [v_d \ v_q]^T$ ;  $\theta = [R_a \ aL_{ad} \ L_q \ L_d]^T$  and  $V = [v_1 \ v_2]^T$  represent the measurement noise.

Using a record of input/output observations  $Y$  and  $H$ ; a recursive estimation procedure [14] is used to estimate the parameter vector  $\theta$ . Initially, it was attempted to estimate the parameter vector  $\theta$ , but this failed to achieve convergence for  $R_a$ . Therefore, because the sensitivity of  $aL_{ad}$ ,  $L_q$  and  $L_d$  estimates is quite negligible even for significant changes in  $R_a$  as shown in Table I, the value of  $R_a$  can be set as the manufacturer's value  $0.0046\Omega$ . However,  $R_a$  will be adjusted by the amount of damping needed, to validate the final model based on simulated against measured responses. Also, the leakage inductance  $L_1$  is assumed to be 9% of  $L_d$ , as given by manufacturer supplied values. Based on this value of  $L_1$ , the turns ratio was calculated to be equal to 15.7621. This assumption on leakage value will also be validated by performing a sensitivity study once the complete model is identified. This tuning procedure is obtained by experience with the measured and manufacturer's data and confidence in their values.

It should be noted that model (7) does not hold during a transient due to the damper winding currents induced in the rotor body. Therefore only steady state portions of the data before and after the disturbance are utilized for estimation. Each portion of the steady state data has a length of 0.235 seconds. The trajectories of recursively estimated parameters can be seen in Fig. 2. The test data in this stage is generated by conducting a small excitation disturbance with the machine operating at light load and under-excited.

## V. ESTIMATION OF SATURATED MUTUAL INDUCTANCES

In this stage of estimation, the saturated mutual inductances  $L_{ads}$  and  $L_{aqs}$  are estimated for each steady state

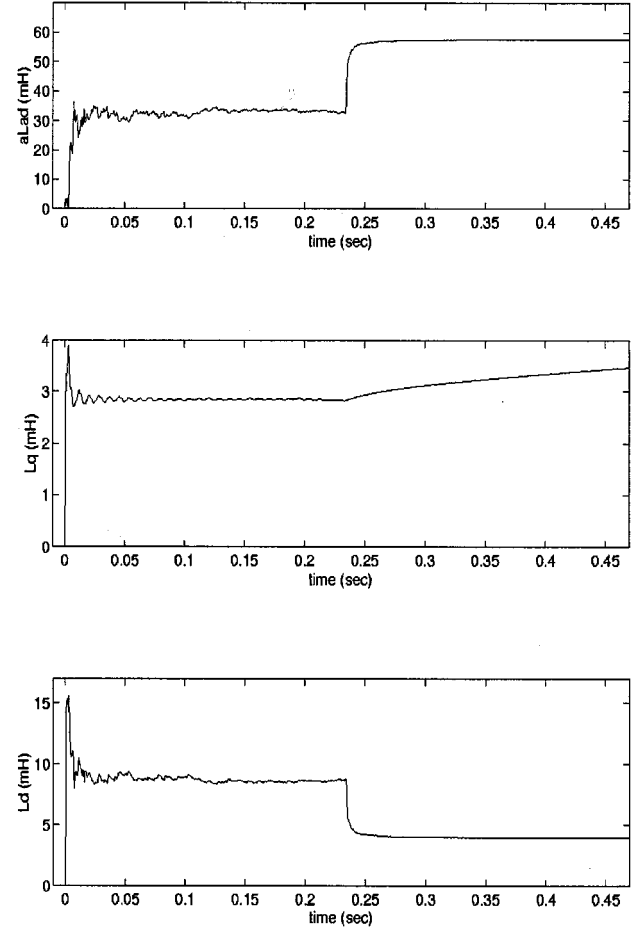


Fig. 2. Recursively estimated parameter trajectories for armature inductances.

data set collected at various levels of excitation and power generation. The subscript "s" denotes a saturated value. Since,  $R_a$  and  $a$  are determined in the previous step, the estimation model can be reformulated as given below,

$$aL_{ad} = a(L_d - L_1) = a(L_d - 0.09L_d) = 0.91aL_d \quad (8)$$

$$\begin{bmatrix} v_{dl} \\ v_{ql} \end{bmatrix} = \begin{bmatrix} \omega_r i_q & 0 \\ 0 & \omega_r (\frac{2}{3}0.91a i_{fd}^* - i_d) \end{bmatrix} \begin{bmatrix} L_{qs} \\ L_{ds} \end{bmatrix} + \begin{bmatrix} v_1 \\ v_2 \end{bmatrix} \quad (9)$$

where  $v_{dl} = v_d + R_a i_d$ ;  $v_{ql} = v_q + R_a i_q$  and  $\theta = [L_{qs} \ L_{ds}]^T$ . Terms  $L_{aqs}$  and  $L_{ads}$  can be extracted from  $L_{ds}$  and  $L_{qs}$  by the same assumption made for  $L_l$ . A total of 28 such steady state data sets were used to identify  $L_{aqs}$  and  $L_{ads}$  by using the recursive maximum likelihood method. It is desirable to graphically visualize the variation of  $L_{aqs}$  and  $L_{ads}$  as a function of all the machine variables ( $v_d, v_q, i_d, i_q, v_{fd}, i_{fd}$ ). However, this is best represented in three dimensions. But if some of the machine variables are considered to be constant, the variation of  $L_{aqs}$  and  $L_{ads}$  can be portrayed in terms of the remaining variables. For example, Fig. 3 depicts the variation of  $L_{aqs}$  and  $L_{ads}$  as a function of power angle, field current, active and reactive power at the machine rated terminal voltage. As can be seen, the  $L_{aqs}$  or  $L_{ads}$  plots look somewhat similar. This can be explained by the

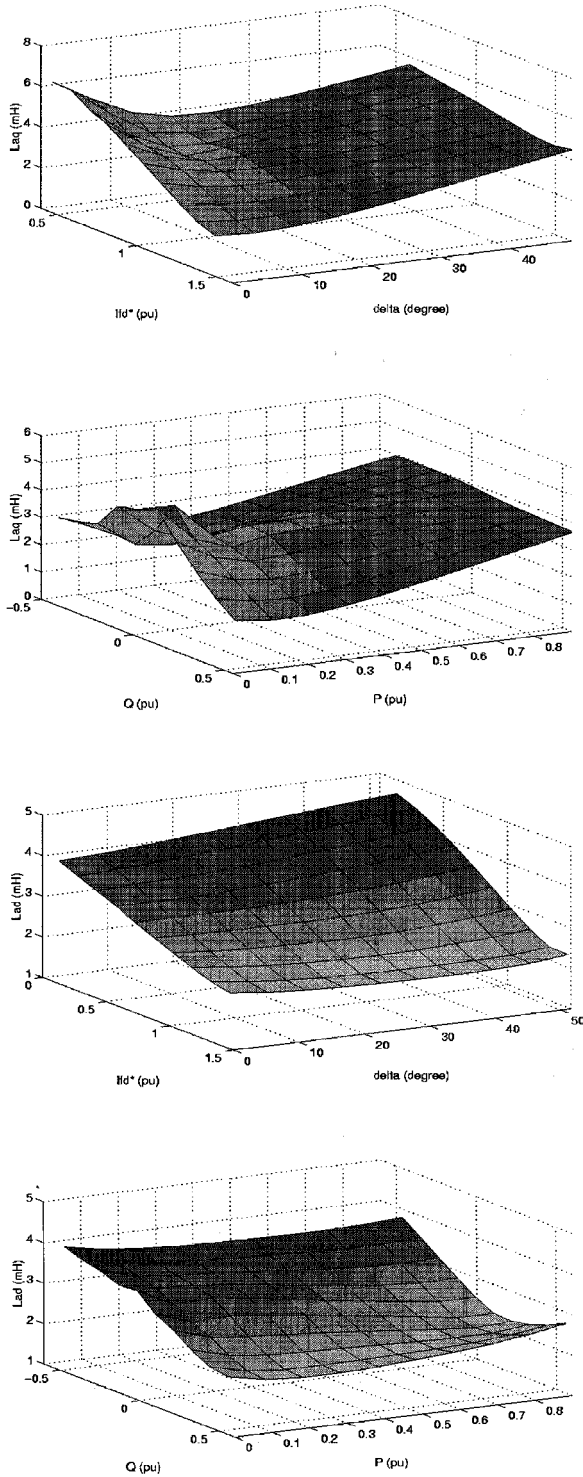


Fig. 3. Variation of saturated mutual inductances as a function of field current  $i_{fd}^*$ , power angle  $\delta$ , active power  $P$  and reactive power  $Q$ .

relationship between variables  $i_{fd}^*$  and  $Q$ , and variables  $\delta$  and  $P$ .

At under-excited conditions, when the generator is delivering small amounts of real power, machine saturation is small. However, at large values of field current and rotor angle when the machine is delivering a substantial amount of real power, the extent of saturation is quite considerable.

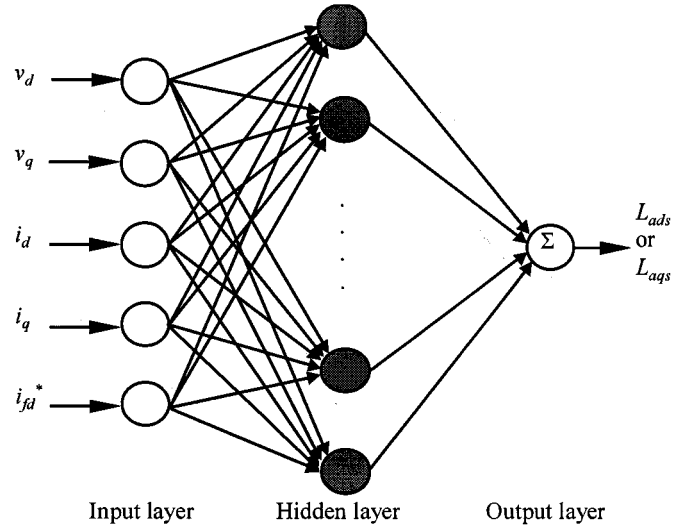


Fig. 4. Multilayer feedforward ANN based saturation model.

## VI. NEURAL NETWORK SATURATION MODEL

The mathematical relationship to be identified between the input and output patterns can be described as

$$\begin{cases} L_{ads} = N_d(v_d v_q i_d i_q i_{fd}^*) \\ L_{aqs} = N_q(v_d v_q i_d i_q i_{fd}^*) \end{cases} \quad (10)$$

where  $N_d$  and  $N_q$  are unknown nonlinear neural network mappings to be established. The field voltage  $v_{fd}^*$  need not be a part of the mapping since it is simply a scaled version of field current  $i_{fd}^*$  at steady state.

The multi-layer feedforward perception has frequently been utilized for system identification studies [15]–[16]. This network consists of a number of basic processing elements with multi-input single-output structure. Every input to the processing element is scaled with a weight, added and mapped to the output through a nonlinear transfer function. The ANN used in this study has three distinct layers: input, hidden, and output and is shown in Fig. 4. The number of processing elements in the hidden layer is arbitrarily chosen depending on the complexity of the mapping. In this study, a hyperbolic tangent transfer function is used in the hidden layer elements while elements in the input and output layers have linear (1:1) transfer functions. The network is trained to minimize the sum squared error function between network outputs and desired actual outputs by adjusting the network weights and biases. The function to be trained can be given as,

$$L_{ais,est} = W_2 \cdot \tanh(W_1 \cdot P + B_1) + B_2 \quad (11)$$

where  $L_{ais,est}$  denotes estimated  $L_{ads}$  or  $L_{aqs}$  and  $P$  is the input pattern. Matrix  $W_1$  is the weight matrix connecting the input and hidden layer elements and has a size of  $m \times 5$ . Matrix  $W_2$  denotes the weight matrix from the hidden layer to the output layer and has a size of  $m \times 1$ .  $B_1$  and  $B_2$  denote the  $m \times 1$  and  $1 \times 1$  bias vectors to the hidden layer and to the output layer respectively. Terms  $W_1$ ,  $W_2$  and  $B_1$ ,  $B_2$  are adjusted to train the network. The training set consists of 20 five-dimensional input patterns. Separate ANN estimators are used to develop  $L_{ads}$  and

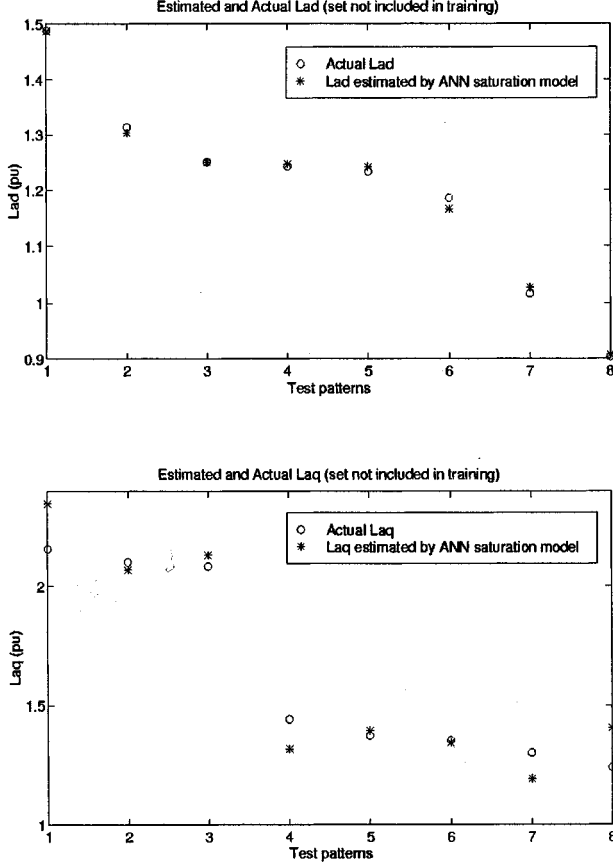


Fig. 5. Actual and ANN estimated generator mutual inductances for the patterns not included in training.

$L_{aqs}$  saturation models. The error goal is set to a value of 0.01. The number of elements in the hidden layer is determined by a trial-and-error procedure.

It was found that an optimal choice for the number of hidden layer elements are 5 for  $L_{ads}$  and 10 for  $L_{aqs}$ . It should be noted that per-unitized values are used in the training instead of actual values to avoid plasticity problems [16].

In order to verify that the networks are able to generalize properly, a cross validation data set, which is not included in the training, is used after the training. Eight such patterns are presented to the trained ANN models. The values of estimated  $L_{ads}$  and  $L_{aqs}$  are compared with the cross validation set not previously used for training. As shown in Fig. 4,  $L_{ads}$  ANN saturation model can correctly interpolate between patterns not used in training. Although, the  $L_{aqs}$  saturation model can not interpolate as well as the  $L_{ads}$  model, it performs reasonably well as shown in Fig. 5. This is probably due to a lack of data in the training process for the  $L_{aqs}$  saturation space. The estimated weights and biases for Lads saturation model can be found in the appendix. Due to space limitations, the weights and biases for the  $q$ -axis saturation model are not given.

## VII. ESTIMATION OF FIELD WINDING AND $D$ -AXIS DAMPER WINDING PARAMETERS

In this section, the estimation procedure involves the identification of field winding and  $d$ -axis damper winding param-

eters. The armature circuit parameters obtained in previous stages are fixed in this estimation procedure. These parameters include  $R_a$ ,  $L_1$ ,  $L_{ad}$  and  $a$ . Then, the parameter vector to be estimated is  $\theta = [R_{fd} \ L_{fd} \ R_{1d} \ L_{1d}]$ .

The model for estimation should first be established. Normally,  $d$ - and  $q$ -axis models are coupled by the speed voltage terms,  $\phi_q \omega_r$  and  $\phi_d \omega_r$  as can be seen in Fig. 1. In order to decouple the model, the voltages  $v_d^*$  and  $v_q^*$  should be computed as follows. The stator voltages in rotor reference frame are,

$$v_d = -R_a i_d - \phi_q \omega_r + p \phi_d \quad (12)$$

$$v_q = -R_a i_q + \phi_d \omega_r + p \phi_q. \quad (13)$$

From (12) and (13) flux dynamics are established as,

$$p \begin{bmatrix} \phi_d \\ \phi_q \end{bmatrix} = \begin{bmatrix} 0 & \omega_r \\ -\omega_r & 0 \end{bmatrix} \begin{bmatrix} \phi_d \\ \phi_q \end{bmatrix} + \begin{bmatrix} v_d + R_a i_d \\ v_q + R_a i_q \end{bmatrix} \quad (14)$$

Once the flux terms are computed using (14), the voltages  $v_d^*$  and  $v_q^*$  can be found as,

$$v_d^* = v_d + \phi_q \omega_r \quad (15)$$

$$v_q^* = v_q - \phi_d \omega_r. \quad (16)$$

Finally, based on  $v_d^*$  the decoupled  $d$ -axis dynamic is,

$$\begin{bmatrix} v_d^* \\ v_{fd} \\ 0 \end{bmatrix} = \begin{bmatrix} -R_a & 0 & 0 \\ 0 & R_{fd} & 0 \\ 0 & 0 & R_{1d} \end{bmatrix} \begin{bmatrix} i_d \\ i_{fd} \\ i_{1d} \end{bmatrix} + \begin{bmatrix} -(L_l + L_{ad}) & aL_{ad}/1.5 & L_{ad} \\ -aL_{ad} & a^2(L_{fd} + L_{ad})/1.5 & aL_{ad} \\ -L_{ad} & aL_{ad}/1.5 & L_{1d} + L_{ad} \end{bmatrix} p \begin{bmatrix} i_d \\ i_{fd} \\ i_{1d} \end{bmatrix} \quad (17)$$

The model (17) is not in the proper form for estimation. To render it amenable for state space representation, it should be rearranged. This is accomplished by taking current vector  $i$  as outputs and voltage vector  $v$  as inputs of the system, then the state space form is,

$$p i = -L^{-1} R i + L^{-1} v. \quad (18)$$

It should be noted that data from large excitation disturbance is required in this stage of estimation. A set of raw measurement data used for this purpose is given in Fig. 6. Table II lists the estimated parameters for a large excitation disturbance data set using model (18) and using Output Error Method of estimation. Fig. 7 illustrates estimated and actual  $i_d$  and  $i_{fd}^*$ .

The agreement between estimated actual curves verifies the accuracy of  $d$ -axis parameters as well as the armature circuit parameters.

## VIII. CONCLUSIONS

A multistage parameter identification procedure involving feed-forward multi-layer ANN based saturation models for a large utility generator is presented. Operating data collected at different levels of excitation and loading conditions are first validated before any estimation procedure. It has been

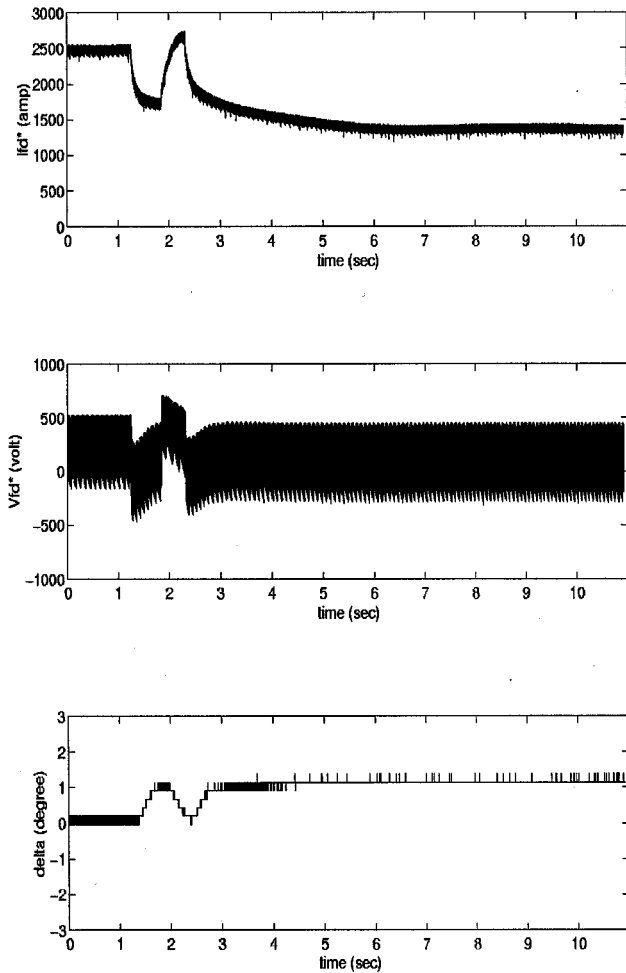


Fig. 6. Raw measurement data for field current  $i_{fd}^*$ , field voltage  $v_{fd}^*$  and power angle  $\delta$ .

TABLE II  
ESTIMATED  $d$ -AXIS PARAMETERS

Parameter	Estimated
$R_{fd}^*$ ( $\Omega$ )	0.1007
$L_{fd}$ (mH)	0.2251
$R_{ld}$ (m $\Omega$ )	0.0132
$L_{ld}$ (mH)	0.9243

observed that  $L_{aq}$  estimates are sensitive to the accuracy of measurements for small angles (i.e. when machine is delivering insignificant amount of real power). A set of small excitation disturbance data is later utilized to estimate armature circuit linear model parameters. Subsequently, saturable inductances  $L_{ads}$  and  $L_{aqs}$  are estimated for each steady state operating point based on the linear model parameters. ANN saturation models are developed by mapping generator terminal variables to  $L_{ads}$  and  $L_{aqs}$  estimates. Validation studies show that ANN models can correctly interpolate between patterns not used in training. It is expected that richer data set collected at different loading and excitation levels would improve the performance of such ANN models. Finally, field winding and damper winding parameters are estimated from large excitation disturbance

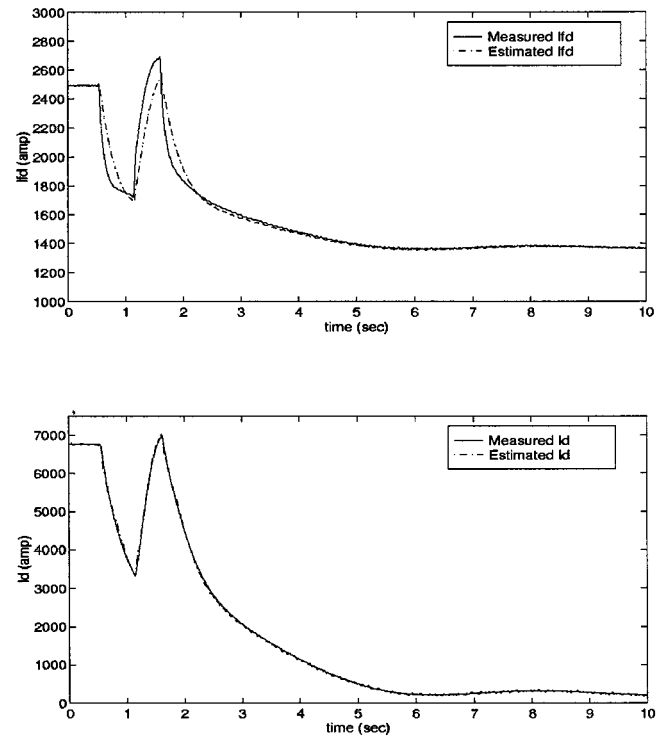


Fig. 7. Estimated and measured  $d$ -axis currents of the machine under large excitation disturbance.

data set. Future work includes the modeling of rotor body parameters for various operating conditions.

#### APPENDIX

#### THE ESTIMATED WEIGHTS AND BIASES FOR $d$ -AXIS ANN SATURATION MODEL

Input to Hidden Layer:

Weights:

$$W1 = \begin{bmatrix} 0.6512 & -0.9691 & -1.0473 & -0.4655 & 0.6278 \\ -1.5023 & -0.6961 & -1.7869 & -1.4397 & -0.4694 \\ 1.3044 & 0.3423 & -0.7986 & 1.4767 & -0.5197 \\ 0.7494 & 1.2630 & 0.2275 & -1.5238 & -1.1039 \\ 0.5208 & -0.7504 & 1.3063 & 0.9582 & -0.3688 \end{bmatrix}$$

Biases:

$$B1^T = [-0.3655 \quad 2.0458 \quad -1.7828 \quad 0.9604 \quad -1.7369]$$

Hidden Layer to Output:

Weights:

$$W2 = [0.4147 \quad 0.0971 \quad -0.9873 \quad 0.9371 \quad 0.4083]$$

Biases:

$$B2 = 0.4353;$$

#### ACKNOWLEDGMENT

The authors acknowledge the assistance of J. Demcko of APS.

## REFERENCES

- [1] *IEEE Guide for Synchronous Generator Modeling Practices in Stability Analysis*, IEEE Std. 1110, 1991.
- [2] A.M. El-Serafi, A.S. Abdallah, M.K. El-Sherbiny, and E.H. Badawy, "Experimental Study of the Saturation and the Cross-Magnetizing Phenomenon in Saturated Synchronous Machines," *IEEE Trans. Energy Conversion*, vol. EC-3, pp. 815–823, Dec. 1988.
- [3] I. Lemay and T.H. Barton, "Small Perturbation Linearization of Saturated Synchronous Machine Equations," *IEEE Trans. Power Apparatus and Systems*, vol. PAS-91, pp. 233–240, 1972.
- [4] G. Shackshaft and P. B. Henser, "Model of Generator Saturation for use in Power System Studies," *Proc. IEE*, vol. 126, no. 8, pp. 759–763, 1979.
- [5] G. Shackshaft and R. Nielson, "Results of Stability Tests on an Under-Excited 120 MW Generator," *Proc. IEE*, vol. 119, pp. 175–188, 1972.
- [6] F. P. De Mello and L.N. Hannett, "Representation of Saturation in Synchronous Machines," *IEEE Trans Power Systems*, vol. 1, pp. 8–14, Nov. 1986.
- [7] A. M. El-Serafi and J. Wu, "Determination of the Parameters Representing the Cross-Magnetizing Effect in Saturated Synchronous Machines," *IEEE Trans. Energy Conversion*, vol. 8, pp. 333–340, Sept. 1993.
- [8] S.H. Minnich, R. P. Schulz, D. H. Baker, D. K. Sharma, R. G. Farmer, and J. H. Fish, "Saturation functions for synchronous generators from finite elements," *IEEE Trans. Energy Conversion*, vol. 2, pp. 680–687, Dec. 1987.
- [9] I. Boldea and S. A. Nassar, "A general equivalent circuit (GEC) of electric machines including crosscoupling saturation and frequency effects," *IEEE Trans. Energy Conversion*, vol. 3, pp. 689–95, Sept. 1988.
- [10] S.A. Tahan and I. Kamwa, "A two factor saturation model for synchronous machines with multiple rotor circuits," *IEEE Trans. Energy Conversion*, vol. 10, no. 4, pp. 609–616, December 1995.
- [11] J. R. Marti and K. W. Louie, "Phase-domain synchronous generator model including saturation effects," *IEEE Trans Power Systems*, vol. 12, no. 1, pp. 222–229, Feb 1997.
- [12] J.-C. Wang, H.-D. Chaing, C.-T. Huang, and Y.-T. Chen, "Identification of synchronous generator saturation based on-line digital measurements," *IEE Proc. Generation, Transmission & Distribution*, vol. 142, no. 3, pp. 225–232, May 1995.
- [13] J. Tamura and I. Takeda, "A New Model of Saturated Synchronous Machines for Power System Transient Stability simulations," *IEEE Trans. Energy Conversion*, vol. 10, no. 2, pp. 218–224, June 1995.
- [14] H. Tsai, A. Keyhani, J.A. Demcko, and R.G. Farmer, "On-line synchronous machine parameter estimation from small disturbance operating data," *IEEE Trans. Energy Conversion*, vol. 10, no. 1, pp. 25–36, Mar. 1995.
- [15] H. Tsai, A. Keyhani, J.A. Demcko, and D.A. Selin, "Development of a Neural Network Saturation Model for Synchronous Generator Analysis," *IEEE Trans. Energy Conversion*, vol. 10, no. 4, pp. 617–624, Dec 1995.
- [16] K.S. Narendra and K. Parthasarathy, "Identification and control of dynamical systems using neural networks," *IEEE Trans. Neural Networks*, vol. 1, pp. 4–27, 1990.
- [17] I.M. Canay, "Causes of Discrepancies on Calculation of Rotor Quantities and Exact Equivalent Diagrams of the Synchronous Machine," *IEEE Trans. PWRs*, vol. PAS-88, no. 7, pp. 1114–1120, July 1969.
- [18] J. L. Kirtley Jr., "On Turbine-Generator Rotor Equivalent Circuit Structures for Empirical Modeling of Turbine Generators," *IEEE Trans.*, vol. PWRs-9, no. 1, pp. 269–271, 1994.
- [19] I. Kamwa, P. Viarouge, and I. Dickinson, "Identification of Generalized Models of Synchronous Machines from Time-Domain Tests," *IEE Proc. C*, vol. 138, no. 6, pp. 485–498, Nov. 1991.
- [20] S. J. Salon, "Obtaining Synchronous Machine Parameters from Test," in *Symposium on Synchronous Machine Modeling for Power Systems Studies*, Piscataway, NJ, USA, Available from IEEE Service Center.
- [21] S.R. Chaudhary, S. Ahmed-Zaid, and N. A. Demerdash, "An artificial neural network model for the identification of saturated turbo-generator parameters based on a coupled finite-element/state-space computational algorithm," *IEEE Trans. Energy Conversion*, vol. 10, pp. 625–633, Dec. 1995.
- [22] J.A. Demcko and J.P. Chrysty, "Self-Calibrating Power Angle Instrument," EPRI, EPRI GS-6475, Research Project 2591-1 Final Report, vol. 2, August 1989.

**H. Bora Karayaka** received the BSEE and MSEE degrees from Istanbul Technical University, Istanbul, Turkey, in 1987 and 1990, respectively. Since 1996, he has been a research associate at The Ohio State University. He is currently working toward his Ph.D. in the Department of Electrical Engineering, The Ohio State University, Columbus, Ohio.

**Ali Keyhani** received Ph.D. degree from Purdue University, West Lafayette, Indiana in 1975. From 1967 to 1969, he worked for Hewlett-Packard Co. on the computer-aided design of electronic transformers. From 1970 to 1973, he worked for Columbus Southern Ohio Electric Co. on computer applications for power system engineering problems. In 1974, he joined TRW Controls and worked on the development of computer programs for energy control centers. From 1976 to 1980, he was a professor of Electrical Engineering at Tehran Polytechnic, Tehran, Iran. Currently, Dr. Keyhani is a Professor of Electrical Engineering at the Ohio State University, Columbus, Ohio. His research interests are in design, control and modeling, parameter estimation, failure detection of electric machines, power electronics and electric drive systems.

**Baj L. Agrawal** was born in Kalaiya, Nepal in 1947. He received his BS in Electrical Engineering from Birla Institute of Technology and Science, India, in 1970 and his Masters and PhD in Control Systems from the University of Arizona, Tucson in 1972 and 1974 respectively. Dr. Agrawal joined Arizona Public Service Company in 1974 where he is currently working as a Senior Consulting Engineer. His responsibilities include dynamic modeling and simulation of power system stabilizer application, power system stability and subsynchronous resonance. Dr. Agrawal has co-authored several papers and a book on subsynchronous resonance published by IEEE. He is registered professional engineer in the state of Arizona and is a member of the IEEE SSR Working Group.

**Douglas A. Selin** was born in Madison, Wisconsin. He received his BSEE in 1983 from Brigham Young University and an ME degree from Rensselaer Polytechnic Institute in 1984. In 1984 he joined Arizona Public Service Company where his responsibilities include subsynchronous resonance problem analysis and simulation of power system dynamics and transients. Mr. Selin is a registered professional engineer in Arizona and a member of Tau Beta Pi and Eta Kappa Nu.

**Gerald Thomas Heydt** is from Las Vegas, Nevada. He holds the BEEE degree from the Cooper Union in New York, and the MSEE and Ph.D. degrees from Purdue University in West Lafayette, Indiana. He was a Professor of Electrical Engineering at Purdue for about 25 years and decided to come back to the West in January, 1996. He presently holds the position of Professor of Electrical Engineering and Center Director for the Center for the Advanced Control of Energy and Power Systems (ACEPS) at Arizona State University in Tempe. He is a registered professional engineer, a member of the National Academy of Engineering, and a Fellow of the IEEE. His interests are electric power quality and computer applications in power engineering.